Study on the Interaction of Cationic Lipids with Bovine Serum Albumin†

David M. Charbonneau and Heidar-Ali Tajmir-Riahi*

Département de Chimie-Biologie, Université du Québec à Trois-Rivières, C. P. 500, Trois-Rivières (Québec), Canada G9A 5H7

Received: October 21, 2009; Revised Manuscript Received: November 11, 2009

There are several lipid binding sites on serum albumins. The aim of this study was to examine the binding of bovine serum albumin (BSA) to cholesterol (Chol), 1,2-dioleoyl-3-(trimethylammonium)propane (DOTAP), (dioctadecyldimethyl)ammonium bromide (DDAB), and dioleoylphosphatidylethanolamine (DOPE), at physiological conditions, using constant protein concentration and various lipid contents. Fourier transform infrared (FTIR), circular dichroism (CD) and fluorescence spectroscopic methods were used to analyze the lipid binding mode, the binding constant, and the effects of lipid complexation on BSA stability and conformation. Structural analysis showed that lipids bind BSA via both hydrophilic and hydrophobic contacts with overall binding constants of $K_{Chol} = (1.12 \pm 0.40) \times 10^3\ M^{-1}$, $K_{DDAB} = (1.50 \pm 0.50) \times 10^3\ M^{-1}$, $K_{DOTAP} = (2.45 \pm 0.80) \times 10^3\ M^{-1}$, and $K_{DOPE} = (1.35 \pm 0.60) \times 10^3\ M^{-1}$. The numbers of bound lipid (n) were 1.1 (cholesterol), 1.28 (DDAB), 1.02 (DOPE), and 1.21 (DOTAP) in these lipid−BSA complexes. DDAB and DOTAP induced major alterations of BSA conformation, causing a partial protein unfolding, while cholesterol and DOPE stabilized protein secondary structure.

Introduction

Serum albumins are the major soluble protein constituents of the circulatory system and have many physiological functions.[1] The most important property of this group of proteins is to serve as transporters for a variety of compounds including fatty acids.[2] There are several lipid binding sites on serum albumins.[3] BSA (Scheme 1) has been one of the most extensively studied of this group of proteins, particularly because of its structural homology with human serum albumin (HSA). The BSA molecule is made up of three homologous domains (I, II, and III) that are divided into nine loops (L1−L9) by 17 disulfide bonds. The loops in each domain are made up of a sequence of large−small−large loops forming a triplet. Each domain in turn is the product of two subdomains (IA, IB, etc.). X-crystallographic data[1,4] show that the albumin structure is predominantly α-helical with the remaining polypeptide occurring in turns and extended or flexible regions between subdomains with no β-sheets. BSA has two tryptophan residues that possess intrinsic fluorescence.[5,6] Trp-134 in the first domain is located on the surface of the molecule, and Trp-212 in the second domain is located within a hydrophobic binding pocket of the protein. While there are marked similarities between BSA and HSA in their compositions, HSA has only one tryptophan residue Trp-214, while BSA contains two tryptophans Trp-212 and Trp-134 as fluorphores capable of fluorescence quenching.[7]

Fluorescence quenching is considered as a technique for measuring binding affinities. Fluorescence quenching is the decrease of the quantum yield of fluorescence from a fluorophore induced by a variety of molecular interactions with quencher molecule.[8] Therefore, it was of interest to use quenching of the intrinsic tryptophan fluorescence of BSA as a tool to study the interaction of cationic lipids with BSA in an attempt to characterize the nature of lipid−protein complexation.

SCHEME 1: Chemical Structure of Bovine Serum Albumin with Tryptophan Residues in Green Color

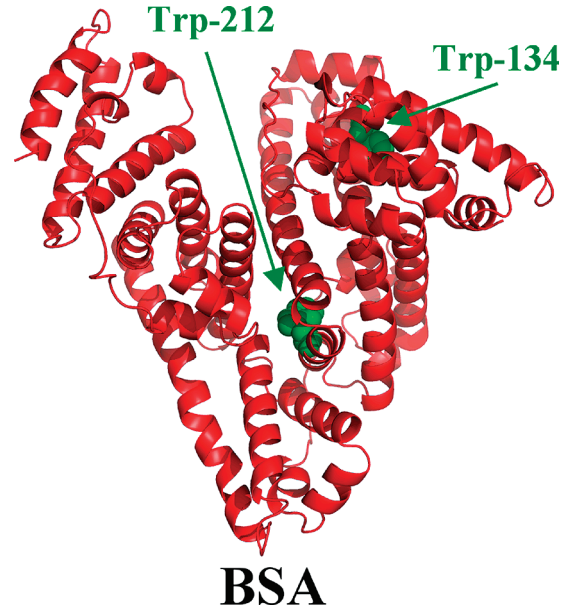

We present spectroscopic analysis of BSA complexes with cholesterol, DOPE, DDAB, and DOTAP (Scheme 2) in aqueous solution at physiological conditions, using constant protein concentration and various lipid concentrations. Structural information regarding lipid binding mode and the effect of lipid−BSA complexation on the protein stability and secondary structure is reported here.

Experimental Section

Materials. BSA fraction V was purchased from Sigma Chemical Co. and used as supplied. Cholesterol, DOTAP,

* To whom correspondence should be addressed. Tel.: 819-376-5011 (ext. 3310). Fax: 819-376-5084. E-mail: tajmirri@uqtr.ca.

† Abbreviations: BSA, bovin serum albumin; Chol, cholesterol; DOTAP, (1,2-dioleoyl-3-trimethylammonium)propane; DDAB, dioctadecyldimethylammonium bromide; DOPE, dioleoylphosphatidylethanolamine; FTIR, Fourier transform infrared spectroscopy; CD, circular dichroism.

10.1021/jp910077h
Published on Web 12/04/2009

SCHEME 2: Chemical Structures of Lipids

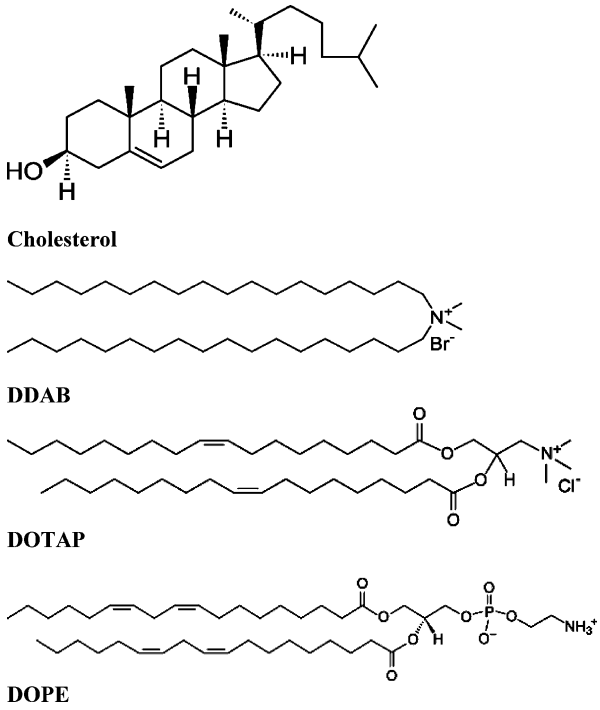

DDAB, and DOPE were from Avanti Polar Lipid Inc. and used as supplied. Other chemicals were of reagent grade and used without further purification.

Preparation of Stock Solutions. Bovine serum albumin was dissolved in aqueous solution (40 mg/mL or 0.5 mM) containing 10 mM Tris-HCl buffer (pH 7.4). The protein concentration was determined spectrophotometrically using the extinction coefficient of 36500 M^{-1} cm^{-1} at 280 nm.[9] A 2 M amount of lipid solution was first prepared in Tris-HCl/ethanol (50%) and then diluted by serial dilution to 1, 0.5, 0.25, and 0.125 mM in Tris-HCl/ethanol (50%). After addition of equal volumes of lipid solution to protein solution, the final ethanol concentration was reduced to 25%. The presence of 25% ethanol induces no major BSA structural changes according to a recent publication.[10] It should be noted that a lipid concentration more than 0.25 mM induced protein precipitation for DDAB and DOTAP, while protein precipitation was not observed for cholesterol and DOPE up to 1 mM lipid content.

FTIR Spectroscopic Measurements. Infrared spectra were recorded on a Fourier transform infrared (FTIR) spectrometer (Impact 420 model), equipped with deuterated triglycine sulfate (DTGS) detector and KBr beam splitter, using AgBr windows. A solution of lipid was added dropwise to the BSA solution with constant stirring to ensure the formation of homogeneous solution and to reach the target lipid concentrations of 0.125, 0.25, 0.5, and 1 mM (for DDAB and DOTAP concentrations were limited to 0.125 and 0.25 mM due to protein precipitation) with a final BSA concentration of 0.25 mM (20 mg/mL). Spectra were collected after 2 h incubation of BSA with lipid solution at room temperature, using hydrated film. Interferograms were accumulated over the spectral range of 600−4000 cm^{-1} with a nominal resolution of 4 cm^{-1} and 100 scans. The difference spectra [(BSA solution + lipid solution) − (BSA solution)] were generated using the polypeptide antisymmetric and symmetric C−H stretching bands,[11] located at 2800−2900 cm^{-1}, as internal standard. The bands due to protein C−H stretching vibrations do not undergo spectral changes (shifting or intensity variation) upon lipid complexation and, therefore, are commonly used as internal standard. For producing difference spectra these bands were adjusted to the baseline level, in order to normalize difference spectra. Details regarding infrared spectral treatment are given in our recent publication.[12]

Analysis of Protein Conformation. Analysis of the secondary structure of BSA and its lipid complexes was carried out on the basis of the procedure previously reported.[13] The protein secondary structure is determined from the shape of the amide I band, located around 1650−1660 cm^{-1}. The FT-IR spectra were smoothed and their baselines were corrected automatically using Grams AI software. Thus the root-mean-square (rms) noise of every spectrum was calculated. By means of the second derivative in the spectral region of 1600−1700 cm^{-1}, six to eight major peaks for BSA and the complexes were resolved. The above spectral region was deconvoluted by the curve-fitting method with the Levenberg−Marquadt algorithm, and the peaks corresponding to α-helix (1656−1658 cm^{-1}), β-sheet (1614−1638 cm^{-1}), turn (1665−1670 cm^{-1}), random coil (1640−1648 cm^{-1}), and β-antiparallel (1680−1692 cm^{-1}) were adjusted and the area was measured with the Gaussian function. The area of all the component bands assigned to a given conformation were then summed up and divided by the total area.[14] The curve-fitting analysis was performed using the GRAMS/AI Version 7.01 software of the Galactic Industries Corp.

Circular Dichroism. Circular dichroism (CD) spectra of BSA and its lipid complexes were recorded with a Jasco J-720 spectropolarimeter. For measurements in the far-UV region (178−260 nm), a quartz cell with a path length of 0.01 cm was used in nitrogen atmosphere. BSA concentration was kept constant (12.5 μM), while each lipid concentration was varied (0.125, 0.25, 0.5, and 1 mM at pH 7.4). DDAB and DOTAP concentrations were limited to 0.025, 0.125, and 0.25 mM due to protein precipitation. An accumulation of five scans with a scan speed of 50 nm/min was performed, and data were collected for each nanometer from 260 to 180 nm. Sample temperature was maintained at 25 °C using a Neslab RTE-111 circulating water bath connected to the water-jacketed quartz cuvettes. Spectra were corrected for buffer signal, and conversion to the Mol CD ($\Delta\varepsilon$) was performed with the Jasco Standard Analysis software. The protein secondary structure was calculated using CDSSTR, which calculates the different assignments of secondary structures by comparison with CD spectra, measured from different proteins for which high-quality X-ray diffraction data are available.[15,16] The program CDSSTR is provided in CDPro software package, which is available at the following Web site: http://lamar.colostate.edu/~sreeram/CDPro.

Fluorescence Spectroscopy. Fluorometric experiments were carried out on a Varian Cary Eclipse. Stock solutions of 2 mM lipid in ethanolic solution were prepared at room temperature (24 ± 1 °C). Various solutions of lipid were prepared from the above stock solutions by successive dilutions also at 24 ± 1 °C. Solution of BSA (10 μM) in 10 mM Tris-HCl (pH. 7.4) was also prepared at 24 ± 1 °C. The above solutions were kept in the dark and used soon after preparation. Samples containing 0.4 mL of the above BSA solution and 0.4 mL of various lipid solutions were mixed to obtain a final lipid concentration of 5−800 μM with constant 5 μM BSA content (in 25% ethanol). The fluorescence spectra were recorded at $\lambda_{exc} = 280$ nm and λ_{em} from 287 to 500 nm. The intensity of the emission band at 334 nm (tryptophan) was used to calculate the binding constant (K) according to literature reports.[17−20]

Molecular Modeling of Bovine Serum Albumin. The structure of BSA was predicted by automated homology

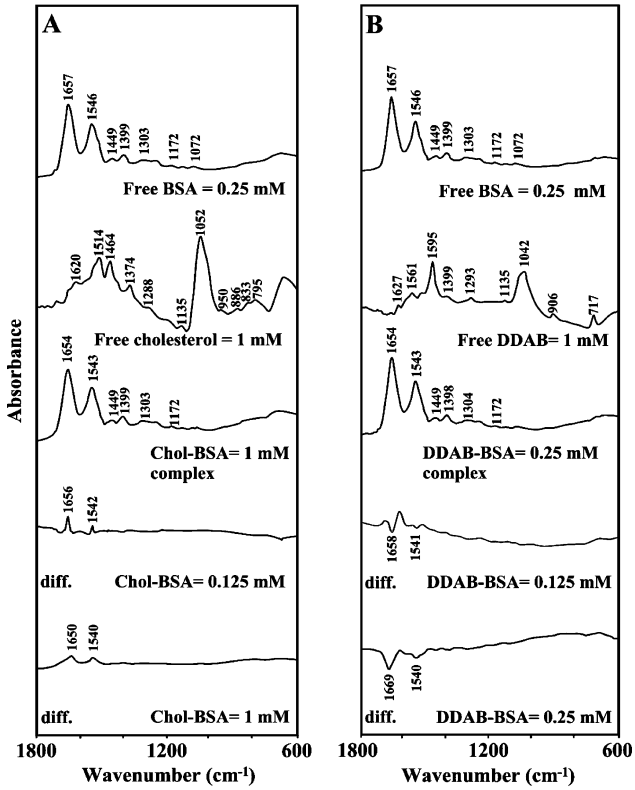

Figure 1. FTIR spectra in the region of 600−1800 cm^{-1} of hydrated films (pH 7.4) for free BSA (0.25 mM), free Chol (1 mM), and Chol−BSA (A) and free DDAB (1 mM) and DDAB−BSA (B; top three curves) and difference spectra (diff.) of lipid−BSA complexes (bottom two curves) obtained at different lipid concentrations (indicated on the figure).

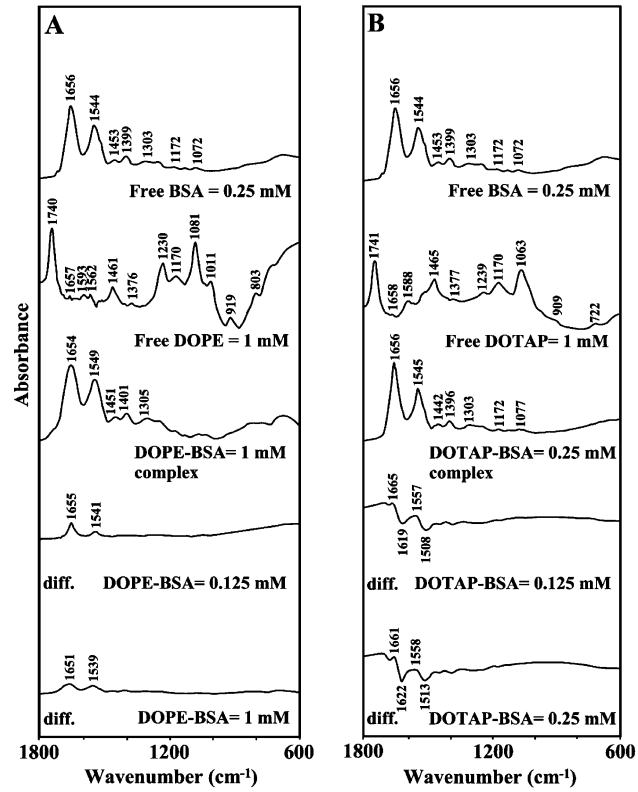

Figure 2. FTIR spectra in the region of 600−1800 cm^{-1} of hydrated films (pH 7.4) for free BSA (0.25 mM), free DOPE (1 mM), and DOPE−BSA (A) and free DOTAP (1 mM) and DOTAP−HSA (B); top three curves) and difference spectra (diff.) of lipid−BSA complexes (bottom two curves) obtained at different lipid concentrations (indicated on the figure).

modeling using SWISS-MODEL Workspace from the amino acid sequence NP-851335.[21,22] The structure of free HSA (PDB id: 1AO6, chain A) obtained by X-ray crystallography was used as a template.[6] These two proteins share 78.1% of sequence identity, which is sufficient to obtain reliable sequence alignment.[23] Images of the structures were generated using Pymol (DeLano Scientific, Palo Alto, CA). The rmsd between model and template proteins was 0.20 Å for positions of backbone atoms, as calculated with DeepView/Swiss-PdbViewer 4.0.1. The quality of the predicted BSA structure was found to be similar to the structure of free HSA used here as a template, using structure and model assessment tools of SWISS-MODEL workspace.

Results and Discussion

Lipid−BSA Interaction by FTIR Spectroscopy. The lipid−BSA complexation was characterized by infrared spectroscopy. Since there was no major spectral shifting for the protein amide I band at 1656 cm^{-1} (mainly C═O stretch) and amide II band at 1544 cm^{-1} (C−N stretching coupled with N−H bending modes)[11−13] upon lipid interaction, the difference spectra [(BSA solution + lipid solution) − (BSA solution)] were obtained, in order to monitor the intensity variations of these vibrations, and the results are shown in Figures 1 and 2. Similarly, the infrared self-deconvolution with second derivative resolution enhancement and curve-fitting procedures[13] were used to determine the protein secondary structure in the presence of lipid (Figure 3 and Table 1).

At low lipid concentration (0.125 mM), intensity changes were observed for the protein amide I at 1657 cm^{-1} and amide II at 1546 cm^{-1}, in the difference spectra lipid−BSA complexes (Figures 1 and 2; difference, 0.125 mM). Positive features are observed in the difference spectra for amide I and II bands at 1655−1656 and 1541−1542 cm^{-1}, Chol−BSA and DOPE−BSA, respectively (Figures 1A and 2A). However, negative features were observed at 1658, 1541 and 1619, 1508 cm^{-1} for DDAB− and DOTAP−BSA, respectively (Figures 1B and 2B). The positive features are related to an increase in the intensity of the amide I and amide II bands upon lipid complexation, while negative features are due to the reduction of intensity of the amide I band due to the loss of protein α helix structure (Figures 1 and 2; difference, 0.125 mM). The spectral changes observed for the amide I and amide II bands (C═O and C−N vibrations) come from lipid−BSA interaction, which aletrs protein conformation. Additional evidence for lipids interaction comes from the shifting of the protein amide A band at 3295 cm^{-1} (N−H stretching mode) in the free BSA to 3299 (Chol−BSA), 3299 (DOPE−BSA), 3297 (DDAB−BSA), and 3298 cm^{-1} (DOTAP−BSA), upon lipid complexation.

As lipid concentration increased to 1 mM, positive features in amide I and II bands were observed at 1651, 1650 (amide I) cm^{-1} and 1539, 1540 cm^{-1} (amide II) for both Chol− and DOPE−BSA complexes, while a major decrease in intensity of the amide I and II bands occurred at 1669, 1540 cm^{-1} and 1661, 1558 cm^{-1} for DDAB− and DOTAP−BSA, respectively (Figures 1 and 2; difference, 1 and 0.25 mM). The observed increase in intensity of the amide I band at 1657 cm^{-1} in the spectra of Chol− and DOPE−BSA suggests a minor alteration, caused by structural changes in intramolecular bonding, while the decrease in the intensity of the amide I band for DDAB− and DOTAP−BSA complexes suggests major protein confor-

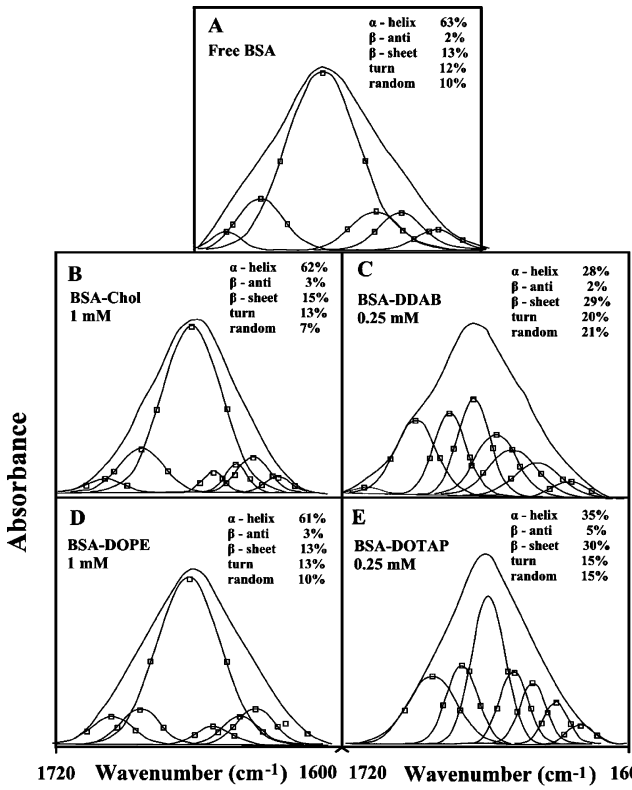

Figure 3. Second derivative resolution enhancement and curve-fitted amide I region (1600−1700 cm^{-1}) for free BSA and its lipid adducts in aqueous solution with 1 mM lipid for Chol and DOPE and 0.25 mM for DDAB and DOTAP with 0.25 mM protein concentrations at pH 7.4.

mational changes upon lipid−protein interaction. Similar infrared spectral changes were observed for the protein amide I band in several drug−protein complexes, where major protein conformational changes occurred.[24] Precipitation of BSA led to increased turbidity when the protein was treated with more than 0.25 mM DDAB and DOTAP (Figures 1 and 2; difference, 0.25 mM).

A quantitative analysis of the protein secondary structure for the free BSA and its lipid adducts in hydrated films has been carried out, and the results are shown in Figure 3 and Table 1. The free protein has 63% α-helix (1657 cm^{-1}), 13% β-sheet (1616, 1625, and 1634 cm^{-1}), 12% turn structure (1677 cm^{-1}), 2% β-antiparallel (1688 cm^{-1}), and 10% random coil (1643 cm^{-1}) (Figure 3A and Table 1). The β-sheet structure is composed of two components at 1616 (intermolecular β-sheet) and 1625 cm^{-1} (intramolecular β-sheet) that are consistent with the spectroscopic data on bovine serum albumin.[25,26] Upon lipid interaction, a minor decrease of α-helix from 63 (free BSA) to 62% (Chol−BSA) and to 61% (DOPE−BSA) with a minor increase of β-sheet from 13% (free BSA) to 15% (Chol−BSA) were observed (Figure 3 and Table 1). However, a major decrease of α-helix was observed from 63 (free BSA) to 28% (DDAB) and to 35% (DOTAP) with an increase in β-sheet structure from 13 (free BSA) to 29% (DDAB) and to 30% (DOTAP), in turn structure from 12 (free BSA) to 20% (DDAB) and to 15% (DOTAP), and in random structure from 10 (free BSA) to 21% (DDAB) and to 15% (DOTAM) (Figure 3 and Table 1). The structural changes suggest important differences in the binding modes of Chol and DOPE compared to DDAB− and DOTAP−protein complexes. The binding of Chol and DOPE led to no major perturbations of BSA conformation and induced protein stabilization, while DDAB and DOTAP complexation caused a partial protein unfolding leading to BSA precipitation at high lipid concentration.

Hydrophobic Interactions. To examine the presence of hydrophobic contacts in lipid−BSA complexes the spectral changes of the lipid antisymmetric and symmetric CH_2 stretching vibrations in the region of 2800−3000 cm^{-1} were monitored by infrared spectroscopy. Free cholesterol CH_2 bands at 2958, 2935, 2899, 2883, 2886, and 2838 cm^{-1} shifted to 2964, 2941, 2912, 2877, and 2834 cm^{-1} (Chol−BSA); free DDAB CH_2 bands at 2951, 2917, and 2847 cm^{-1} shifted to 2959, 2914, and 2870 cm^{-1} (DDAB−BSA); free DOTAP at 2956, 2925, and 2854 cm^{-1} shifted to 2958, 2932, and 2872 cm^{-1} (DOTAP−BSA); and free DOPE at 2953, 2925, and 2854 cm^{-1} shifted to 2960, 2927, and 2852 cm^{-1} (DOPE−BSA) in the lipid−protein complexes (Figure 4). The shifting of the lipid antisymmetric and symmetric CH_2 stretching vibrations in the region of 2800−3000 cm^{-1} of the infrared spectra suggests the presence of hydrophobic interactions via lipid aliphatic tails and the hydrophobic region in BSA. The observed spectral shifting for the lipid CH_2 stretching modes is consistent with a major hydrophobic interaction via lipid aliphatic tails. However, hydrophilic interactions for lipid−BSA complexes were also observed by the intensity variations of the protein C═O and C−N stretching bands (amide I and amide II bands) in the region of 1500−1700 cm^{-1}, described in infrared discussion (Figures 1 and 2).

CD Spectra. The CD spectroscopic results for BSA and its lipid complexes shown in Figure 5 and Table 2 exhibit marked similarities with those of the infrared data. Secondary structure analysis based on CD results suggests that free BSA has a high α-helix content (62%), with 7% β-sheet, 12% turn, and 19% random (Figure 5 and Table 2), which is consistent with the literature report.[25,26] Upon lipid complexation, minor changes in α-helix were observed from 62% free protein to 65% for Chol−BSA and 61% for DOPE−BSA complexes (Figure 5 and Table 2). However, major reduction of the α-helix from 62 (free BSA) to 33% (DOTAP−BSA) and to 30% (DDAB−BSA) was observed, concomitant with a major increase in β-sheet from 7 (free BSA) to 22% and to 25% for DOTAP− and DDAB−BSA complexes, respectively (Figure 5 and Table 2). Similarly, turn and random structures

TABLE 1: Secondary Structure Analysis (Infrared Spectra) for the Free BSA and Its Lipids Complexes in Hydrated Film at pH 7.4 (with the Margin of Error ±1 to ±3%)

	secondary structure analysis (%)				
amide I components (cm^{-1})	free BSA (0.25 mM)	Chol−BSA (1 mM)	DDAB−BSA (0.25 mM)	DOTAP−BSA (0.25 mM)	DOPE−BSA (1 mM)
1680−1692 β-anti	2	3	2	5	3
1660−1680 turn	12	13	20	15	13
1650−1660 α-helix	63	62	28	35	61
1641−1648 random coil	10	7	21	15	10
1610−1640 β-sheet	13	15	29	30	13

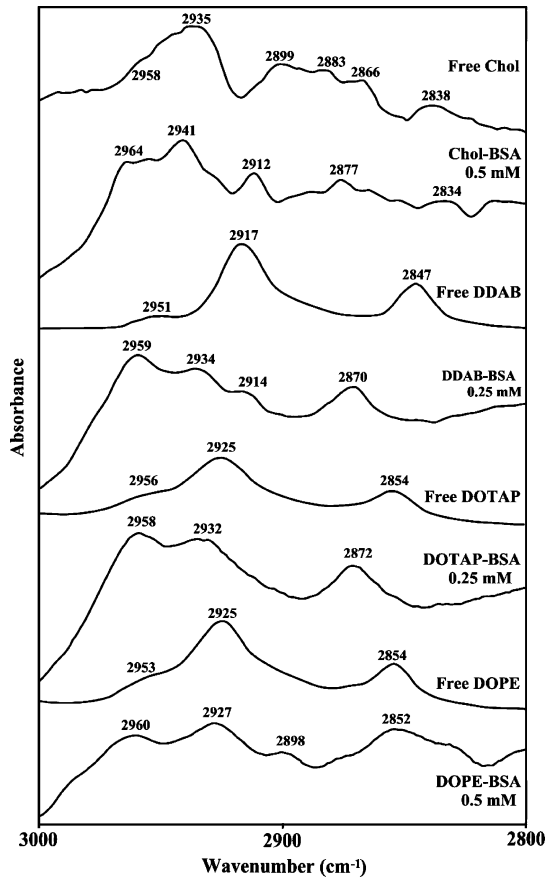

Figure 4. Spectral changes of lipid CH_2 symmetric and antisymmetric stretching vibrations upon BSA complexation (the contribution from free protein vibrations has been subtracted in this region).

were increased, upon DDAB− and DOTAP−protein complexation (Figure 5 and Table 2). The CD data related to conformational changes of lipid−BSA are consistent with the infrared results that showed no major alterations of α-helix for Chol− and DOPE−BSA adducts, while a major reduction of α-helix occurred for DDAB− and DOTAP−BSA complexes in favor of an increase in β-sheet, turn, and random coil structures (Tables 1 and 2). The considerable conversion of α-helix to β-sheet, turn, and random structures in DDAB and DOTAP complexes can be related to precipitation due to the protein denaturation. This can occur via intermolecular β-sheet formation, which may in turn lead to interprotein sheet structure.[27] The conformational changes observed via CD and IR results are indicative of a partial protein unfolding in the DDAB− and DOTAP−BSA complexes, while some degree of stabilization is induced by Chol− and DOPE−BSA adduct formation. It should be noted that a major reduction of intensity signal observed in CD spectra of DDAB−BSA and DOTAP−BSA (0.25 mM), is due to precipitation of lipid−protein complexes as the turbidity of solution was observed in the cuvette (Figure 5B,C, 0.25 mM).

Fluorescence Spectra and Stability of Lipid−BSA Complexes. BSA has two tryptophan residues that possess intrinsic fluorescence:[7] Trp-212 is located within a hydrophobic binding pocket of the protein, while Trp-134 is located on the surface of the molecule (Scheme 2). Tryptophan emission dominates BSA fluorescence spectra in the UV region. When other molecules interact with BSA, tryptophan fluorescence may change depending on the impact of such interaction on the

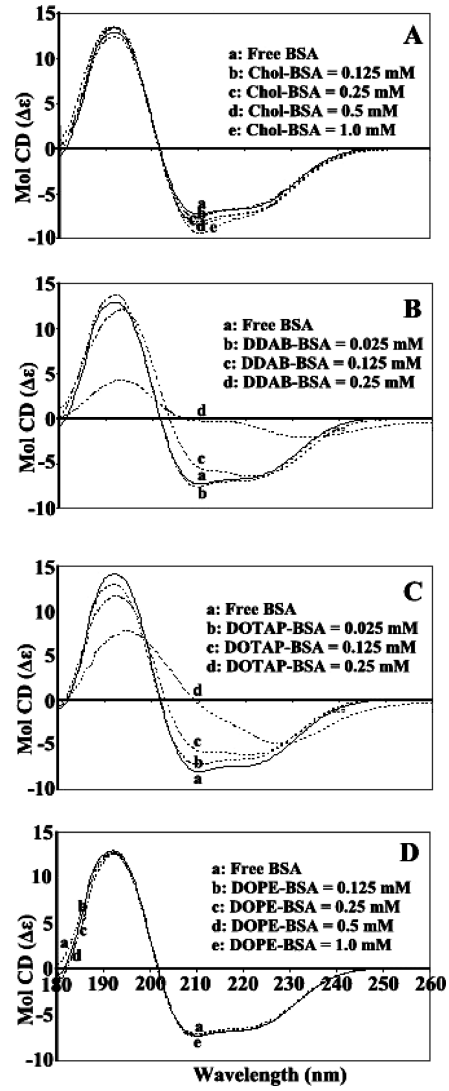

Figure 5. Circular dichroism of free BSA and its lipid complexes in aqueous solution with protein concentration of 12.5 μM and lipid concentrations of 0.025, 0.125, and 0.25 for DDAB and DOTAP and from 0.125 0.25, 0.50, and 1 mM for cholesterol and DOPE in 5 mM Tris-HCl buffer pH 7.4, 25% ethanol (v/v) at 25 °C.

TABLE 2: Secondary Structure of BSA Complexes (CD Spectra) with Lipids at pH 7.4. Calculated by CDSSTR Software

complex (lipid concentration (mM))	α-helix (±3%)	β-sheet (±2%)	turn (±2%)	random (±2%)
free BSA	62	7	12	19
Chol−BSA (1 mM)	65	5	12	18
DOPE−BSA (1 mM)	61	7	14	18
DOTAP−BSA (0.25 mM)	33	22	19	26
DDAB−BSA (0.25 mM)	30	25	25	20

protein conformation.[8] On the assumption that there are (n) substantive binding sites for quencher (Q) on protein (B), the quenching reaction can be shown as follows:

$$n\mathrm{Q} + \mathrm{B} \leftrightarrow \mathrm{Q}_n\mathrm{B} \quad (1)$$

The binding constant (K_A) can be calculated as

$$K_A = [\mathrm{Q}_n\mathrm{B}]/[\mathrm{Q}]^n[\mathrm{B}] \quad (2)$$

where [Q] and [B] are the quencher and protein concentrations, respectively, [Q_nB] is the concentration of nonfluorescent

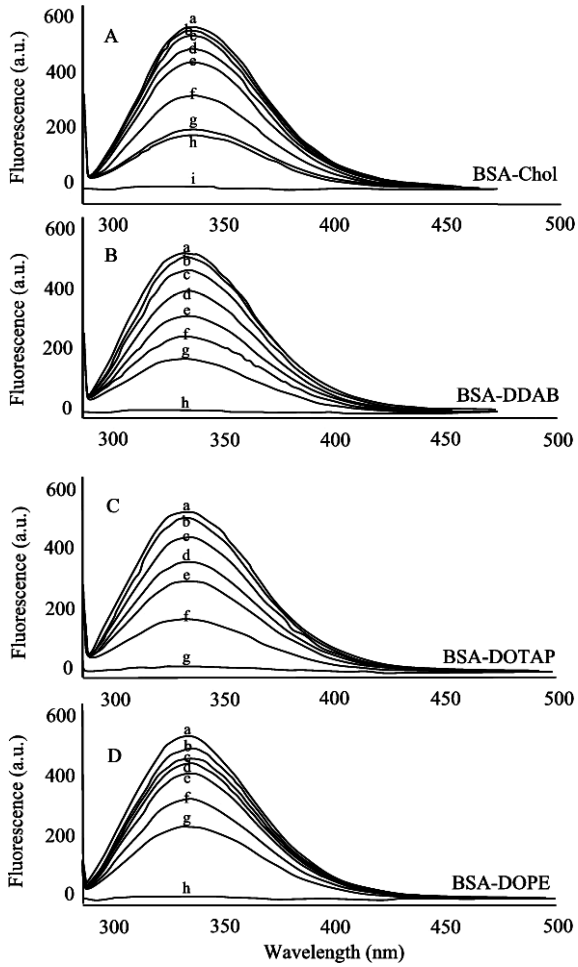

Figure 6. Fluorescence emission spectra of lipid−BSA systems in 10 mM Tris-HCl buffer pH 7.4, 25% ethanol at 25 °C for (A) Chol−BSA [(a) free BSA (5 μM), (b−h) BSA 5 μM with Chol at 20, 50, 60, 90, 200, 400, and 800 μM, and i) 1 mM free cholesterol], (B) DDAB−BSA [(a) free BSA (5 μM), (b−g) DDAB at 10, 50, 80, 100, 200, and 400 μM and (h) 1 mM free DDAB], (C) DOTAP−BSA [(a) free BSA (5 μM), (b−f) DOTAP at 10, 50, 80, 100, and 200 μM, and (g) 1 mM free DOTAP], and (D) DOPE−BSA [(a) free BSA (5 μM), (b−g) DOPE at 10, 50, 80, 100, 200, 300, and 400 μM, and (h) 1 mM free DOPE].

fluorophore−quencher complex, and $[B_0]$ gives the total protein concentration:

$$[Q_nB] = [B_0] - [B] \quad (3)$$

$$K_A = [B_0] - [B]/[Q]^n[B] \quad (4)$$

The fluorescence intensity is proportional to the protein concentration as described by

$$[B]/[B_0] \propto F/F_0 \quad (5)$$

Results from fluorescence measurements can be used to estimate the binding constant of the lipid−protein complex. From eq 4

$$\log[(F_0 - F)/F] = \log K_A + n \log[Q] \quad (6)$$

The accessible fluorophore fraction (f) can be calculated by modified Stern−Volmer equation:

$$F_0/(F_0 - F) = 1/fK[Q] + 1/f \quad (7)$$

where F_0 is the initial fluorescence intensity and F is fluorescence intensities in the presence of quenching agent (or interacting molecule). The plot of log[$(F_0 - F)/F$] vs log[lipid]

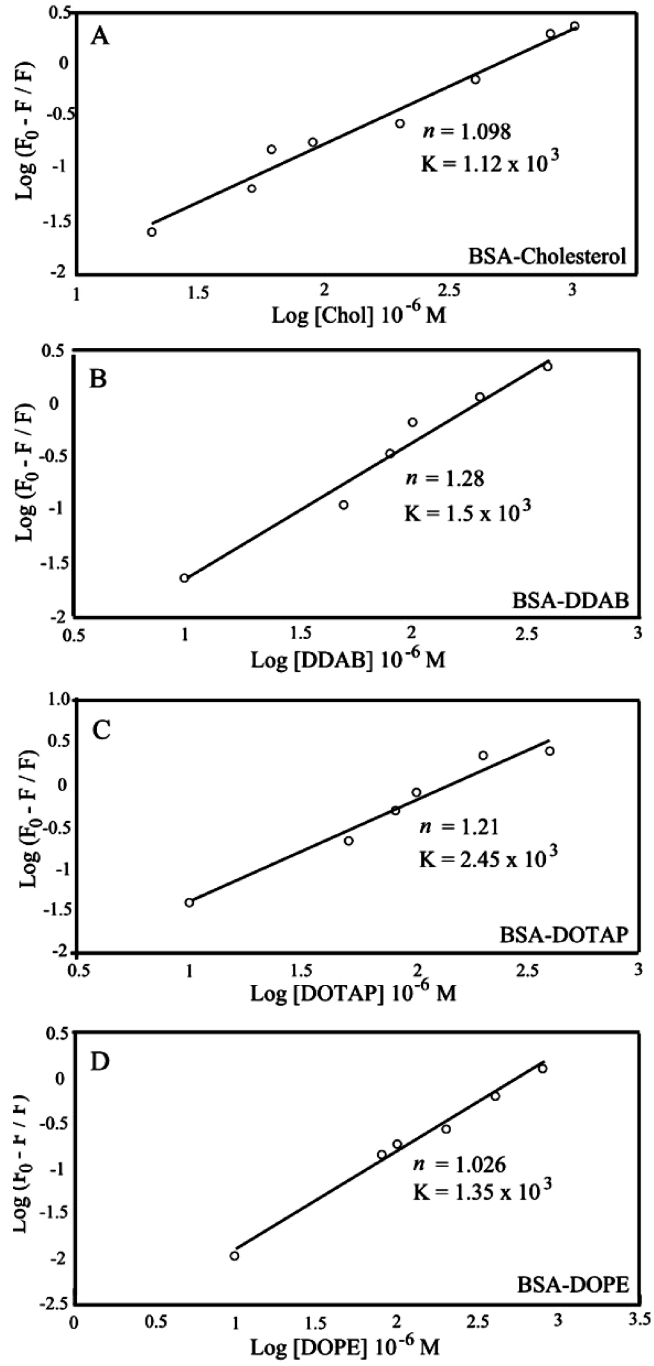

Figure 7. Plot of log[$(F_0 - F)/F$] as a function of log[lipid]. The binding constant K being the antilog of the intercept (A) Chol−BSA, (B) DDAB−BSA, (C) DOTAP−BSA, and (D) DOPE−BSA complexes with the number of bound lipid (n).

yield log K_s as the intercept on the y axis and n as the slope.[8] Thus, the antilog of the intercept gives K_s. The decrease of fluorescence intensity of BSA is monitored at 334 nm for BSA−lipid systems (parts A−D of Figure 6 show representative results for each system). Parts A−D of Figure 7 show representative plots of log[$(F_0 - F)/F$] vs log[lipid].

Assuming that the observed changes in fluorescence come from the interaction between lipid and BSA, the quenching constant can be taken as the binding constant of the complex formation.[28] The resulting emission λ_{max} for BSA was at 334 nm. We predict that lipid interaction with BSA results in quenching effect with the two fluorophores Trp-212 buried inside and Trp-134 located on the surface of BSA. The changes

in fluorescence intensity of Trp-212 and Trp-134 in the presence of lipid may arise as a direct quenching or as a result of protein conformational changes induced by lipid−BSA complexation. However, the results indicated that lipid interaction do not change the emission λ_{max} at 334 nm. No spectral shifting was observed for the emission spectra upon lipid−BSA complexation, indicating that tryptophan molecules are not exposed to any change in polarity. Both hydrophobic and hydrophilic interactions were suggested for lipid−BSA complexes. The K values given here are averages of four-replicate and six-replicate runs for BSA/lipid systems, each run involving several different concentrations of lipid (Figure 7). The order of lipid binding is DOTAP > DDAB > DOPE > Chol with $K_{Chol} = (1.12 \pm 0.40) \times 10^3\ M^{-1}$, $K_{DDAB} = (1.50 \pm 0.50) \times 10^3\ M^{-1}$, $K_{DOTAP} = (2.45 \pm 0.80) \times 10^3\ M^{-1}$, and $K_{DOPE} = (1.35 \pm 0.60) \times 10^3\ M^{-1}$ (Figure 7A−D). The association constants calculated for the lipid−BSA show low-affinity lipid−protein binding, compared to the other strong ligand−protein complexes with binding constants ranging from 10^5 to $10^8\ M^{-1}$.[29,30] However, lower binding constants (10^4 to $10^5\ M^{-1}$) were recently reported for several ligand−protein complexes by fluorescence spectroscopy, consistent with our results.[17−20] The present interpretation is supported by the binding constants obtained for different lipid−BSA complexes. Indeed, the binding constants calculated from fluorescence data show stronger affinity for DOTAP and DDAB than those of the Chol−and DOPE−protein adducts with the order of DOTAP > DDAB > DOPE > Chol (Figure 7). The results obtained from these different spectroscopic methods consistently show that major perturbations of protein secondary structure occurred by DDAB and DOTAP and that they are involved in different binding modes from those of the Chol− and DOPE−protein complexes.

The number of ligands bound (n) can be calculated from $\log[(F_0 - F)/F] = \log K_S + n \log[\text{lipid}]$ for the static quenching.[31−33] From the linear plots of $\log[(F_0 - F]/F]$ as a function of log[lipid] is shown in Figure 7, the n values from the slopes of the straight line are 1.09 (cholesterol), 1.28 (DDAB), 1.21 (DOTAP), and 1.02 (DOPE) (Figure 7A−D). The larger bindings observed for DDAB ($n = 1.28$) and DOTAP ($n = 1.21$) are consistent with major perturbations of BSA secondary structure inducing protein unfolding. The binding sites of cholesterol and DOPE seem to be different from those of DDAB and DOTAP in which lipid complexation causes more impact on BSA conformation than DOPE and cholesterol. The different binding modes of Chol and DOPE compared to DDAB and DOTAP may be due to neutral forms of lipids (helper) with weaker protein interaction (smaller K values) than those of cationic lipid complexes.

Comparison between Lipid−BSA and Lipid−HSA Complexes. HSA and BSA are homologue proteins showing ~76% of sequence identity. BSA contains two tryptophan residues (Trp-212 and Trp-134), while HSA has only one tryptophan (Trp-214). The BSA three-dimensional structure is very similar to that of HSA as suggested by the 3D modeling presented here (Scheme 1). Our spectroscopic results showed that lipids bind to BSA via both hydrophilic and hydrophobic interactions as previously suggested for HSA.[33] In both cases, a partial protein unfolding occurred for HSA and BSA in the presence of DDAB and DOTAP, while cholesterol and DOPE did not change the protein conformation and seem to induced structural stabilization. Results from fluorescence showed also the similarity between interaction profiles of lipids with BSA and HSA. The order of lipid−BSA binding was DOTAP > DDAB > DOPE > Chol with $K_{Chol} = 1.12 \times 10^3\ M^{-1}$, $K_{DDAB} = 1.50 \times 10^3\ M^{-1}$, $K_{DOTAP} = 2.45 \times 10^3\ M^{-1}$, and $K_{DOPE} = 1.35 \times 10^3\ M^{-1}$. However, stronger lipid−HSA interaction was observed with the binding constants of $K_{chol} = 2.3 \times 10^3\ M^{-1}$ and $K_{DDAB} = 8.9 \times 10^3\ M^{-1}$, $K_{DOPTAP} = 9.1 \times 10^3\ M^{-1}$, and $K_{DOPE} = 4.70 \times 10^3\ M^{-1}$.[33] A larger number of bound lipid (n) was found for HSA with Chol ($n = 1.22$), DDAB ($n = 1.82$), DOTAP ($n = 1.56$), and DOPE ($n = 1.76$)[33] than those of lipid−BSA complexes with Chol ($n = 1.1$), DDAB ($n = 1.28$), DOTAP ($n = 1.21$), and DOPE ($n = 1.02$) studied here. This result can be attributed to differences in the quenching effect on the Trp-214 pocket buried inside HSA, compared to lipid quenching in BSA which occurs partly with the Trp-134 in the surface as well as the Trp-212 inside the protein. In conclusion the cationic lipids interaction with BSA and HSA showed important similarity such as partial protein unfolding for DDAB and DOTAP complexes characterized by a major $\alpha \rightarrow \beta$ transition, while cholesterol and DOPE induced protein stabilization. Helper lipids, cholesterol and DOPE, do not affect HSA and BSA structures due to a different binding mode than those of the cationic lipids DDAB and DOPTAP.

Acknowledgment. This work is supported by a grant from the Natural Sciences and Engineering Research Council of Canada (NSERC). D.M.C. acknowledges a studentship from PROTEO, Université Laval.

References and Notes

(1) Peters. T. *All about Albumin. Biochemistry, Genetics and Medical Applications*; Academic Press: San Diego, CA, 1996.
(2) Simard, J. R.; Zunszain, P. A.; Ha, C. E.; Yang, J. S.; Bhagavan, N. V.; Petitpas, I.; Curry, S.; Hamilton, J. A. *Proc. Natl. Acad. Sci. U.S.A.* **2005**, *102*, 17958–17963.
(3) Bhattacharya, A. A.; Grune, T.; Curry, S. *J. Mol. Biol.* **2000**, *303*, 721–732.
(4) He, X. M.; Carter, D. C. *Nature* **1992**, *358*, 209–215.
(5) Peters, T. *Adv. Protein Chem.* **1985**, *37*, 161–245.
(6) Sugio, S.; Kashima, A.; Mochizuki, S.; Noda, M.; Kobayashi, K. *Protein Eng.* **1999**, *12*, 439–446.
(7) Tayeh, N.; Rungassamy, T.; Albani, J. R. *J. Pharm. Biomed. Anal.* **2009**, *50*, 107–116.
(8) Lakowicz, J. R. *Principles of Fluorescence Spectroscopy*, 2nd ed.; Kluwer/Plenum: New York, 1999.
(9) Painter, L.; Harding, M. M.; Beeby, P. J. *J. Chem. Soc., Perkin Trans.* **1998**, *18*, 3041–3050.
(10) Lin, S. Y.; Li, M. J.; Wei, Y. S. *Spectrochim. Acta, Part A* **2004**, *60*, 3107–3111.
(11) Krimm, S.; Bandekar, J. *Adv. Protein Chem.* **1986**, *38*, 181–364.
(12) Beauchemin, R.; N' soukpoe-Kossi, C. N.; Thomas, T. J.; Thomas, T.; Carpentier, R.; Tajmir-Riahi, H. A. *Biomacromolecules* **2007**, *8*, 3177–3183.
(13) Byler, D. M.; Susi, H. *Biopolymers* **1986**, *25*, 469–487.
(14) Ahmed, A.; Tajmir-Riahi, H. A.; Carpentier, R. *FEBS Lett.* **1995**, *363*, 65–68.
(15) Johnson, W. C. *Proteins: Struct., Funct. Genet.* **1999**, *35*, 307–312.
(16) Sreerama, N.; Wody, R. W. *Anal. Biochem.* **2000**, *287*, 252–260.
(17) Tang, J.; Qi, S.; Chen, X. *J. Mol. Struct.* **2005**, *779*, 87–95.
(18) Bi, S.; Ding, L.; Tian, Y.; Song, D.; Zhou, X.; Liu, X.; Zhang, H. *J. Mol. Struct.* **2004**, *703*, 37–45.
(19) He, W.; Li, Y.; Xue, C.; Hu, Z.; Chen, X.; Sheng, F. *Bioorg. Med. Chem.* **2005**, *13*, 1837–1845.
(20) Dufour, C.; Dangles, O. *Biochim. Biophys. Acta* **2005**, *1721*, 164–173.
(21) Arnold, K.; Bordoli, L.; Kopp, J.; Schwede, T. *Bioinformatics* **2006**, *22*, 195–201.
(22) Rost, B. *Protein Eng.* **1999**, *12*, 85–94.
(23) Schwede, T.; Kopp, J.; Guex, N.; Peitsch, M. C. *Nucleic Acids Res.* **2003**, *31*, 3381–3385.
(24) Ahmed Ouameur, A.; Diamantoglou, S.; Sedaghat-Herati, M. R.; Nafisi, Sh.; Carpentier, R.; Tajmir-Riahi, H. A. *Cell Biochem. Biophys.* **2006**, *45*, 203–213.
(25) Tian, J.; Liu, J.; Zhide Hu, Z,; Xingguo Chen, X. *Am. J. Immunol.* **2005**, *1*, 21–23.
(26) Grdadolnik, J. *Acta Chim. Slov.* **2003**, *50*, 777–788.

(27) Harrison, R. S.; Sharp, P. C.; Singh, Y.; Fairlie, D. P. *Rev. Physiol., Biochem. Pharmacol.* **2007**, *159*, 1–10.
(28) Liu, J.; Tian, J.; Hu, Z.; Chen, X. *Biopolymers* **2004**, *73*, 443–450.
(29) Kragh-Hansen, U. *Dan. Med. Bull.* **1990**, *37*, 57–84.
(30) Kratochwil, N. A.; Huber, W.; Muller, F.; Kansy, M.; Gerber, P. *R. Biochem. Pharmacol.* **2002**, *64*, 1355–1374.
(31) Dockal, M.; Chang, C.; Carter, D. C.; Ruker, F. *J. Biol. Chem.* **2000**, *275*, 3042–3050.
(32) Liang, L.; Tajmir-Riahi, H. A.; Subirade, M. *Biomacromolecules* **2008**, *9*, 50–55.
(33) Charbonneau, D.; Beauregard, M.; Tajmir-Riahi, H. A. *J. Phys. Chem. B* **2009**, *113*, 1777–1783.

JP910077H